Translational Oncology
www.transonc.com

Volume 10 Number 1 February 2017 pp. 46–53 46

Arterial Phase with CAIPIRINHA-Dixon-TWIST (CDT)–Volume-Interpolated Breath-Hold Examination (VIBE) in Detecting Hepatic Metastases

Jinrong Qu*, Shuai Han*, Hongkai Zhang*, Hui Liu†, Zhaoqi Wang*, Ihab R. Kamel‡, Kiefer Berthold§, Nickel Marcel Dominik§, Jianwei Zhang*, Shouning Zhang*, Yafeng Dong*, Lina Jiang*, Cuicui Liu* and Hailiang Li*

*Department of Radiology, the Affiliated Cancer Hospital of Zhengzhou University, Henan Cancer Hospital, Zhengzhou, China, 450008; †MR Collaboration, Siemens Healthcare, Shanghai, China, 201318; ‡Department of Radiology, Johns Hopkins University School of Medicine, Baltimore, MD, USA, 21205-2196; §MR Pre-development, Siemens Healthcare, Erlangen, Germany, 91052

Abstract

PURPOSE: To evaluate lesion enhancement performance of Multi-Arterial CAIPIRINHA-Dixon-TWIST–Volume-Interpolated Breath-Hold Examination (MA-CDT-VIBE) for the detection of hepatic metastases. *MATERIALS AND METHODS:* Thirty-one patients with suspicious hepatic metastases were enrolled in this retrospective study. Two independent radiologists scored visualization of each lesion on a scale of 1 (poor visualization) to 11 (excellent visualization) on 11 sets of images. These included 6 hepatic arterial sub-phases acquired in one breath-hold, 1 series of the mean of 6 hepatic arterial sub-phases, 3 subtracted arterial sub-phases, and 1 portal venous phase. The phases with good (score 8–10) and excellent (score 11) lesion visualization were identified, and the number of lesions seen on each of these phases was compared to the number of lesions that was seen best on the equivalent-to-conventional single arterial phase as well as to those that were see best on the mean of 6 hepatic arterial sub-phases. Inter-reader agreement was also calculated. *RESULTS:* The MA-CDT-VIBE was successfully acquired in 25 patients with hypervascular metastases (96 lesions) and 6 patients with hypovascular metastases (13 lesions). In case of hypervascular metastases, the 6th/6 arterial sub-phase had excellent lesion visualization (sore of 11) in 56 and 44 lesions for the 2 readers, respectively. Good lesion visualization (score of 8-10) was recorded in 5th/6 arterial subphases, in 81 and 67 lesions for the 2 readers, respectively. In case of hypovascular metastases, the portal venous phase had excellent lesion visualization (sore of 11) in all 13 lesions for the 2 readers. Good lesion visualization (score of 8–10) was recorded in 12 and 13 lesions on the 5th/6 and 6th/6 arterial subphases, respectively. More hypervascular lesions scored good (score of 8–10) and excellent (score of 11) on the 5th/6 and 6th/6 phases of MA-CDT-VIBE compared with the equivalent-to-conventional single arterial phase (3rd/6) and the set with mean of 6 hepatic arterial sub-phases. The results were statistically significant (*t* test, $P < .0001$). Inter-reader agreement was good for hypervascular lesions (kappa = 0.627, $P < .0001$) and excellent for hypovascular lesions (kappa = 1.0, $P < .0001$), respectively. *CONCLUSIONS:* The MA-CDT-VIBE improves lesion conspicuity by providing a wide observation window for hypervascular lesions. For hypovascular lesions, the advantage of multiple arterial sub-phases over the portal venous phase is not apparent.

Translational Oncology (2017) 10, 46–53

Introduction

Partial hepatic resection is a well accepted procedure in the management of early hepatic metastases [1]. It is essential for adequate surgical planning and successful hepatic resection to accurately assess the number, size, and location of the lesions as well as the number of involved liver segments [2,3]. A meta-analysis

Address all correspondence to: Jinrong Qu or Hailiang Li, Department of Radiology, the Affiliated Cancer Hospital of Zhengzhou University, Henan Cancer Hospital, Zhengzhou, China, 450008.
E-mail: qjryq@126.com
Received 26 September 2016; Revised 14 November 2016; Accepted 14 November 2016

1936-5233/17
http://dx.doi.org/10.1016/j.tranon.2016.11.005

of prospective studies demonstrated a superior performance of MRI over FDG-PET and CT on a lesion-by-lesion basis in the detection of hepatic metastases and in particular for lesions less than 1 cm in size (sensitivity 80%-88% and specificity 93%-97%) [4]. The reported sensitivity of hepatocyte specific contrast enhanced MRI for the detection of hepatic metastases ranged between 91% and 97% compared with 71% and 73.5% for CT [5–7]. The reported sensitivity of hepatocyte-specific contrast agents in the detection of hepatic metastases from gastrointestinal malignancies was significantly improved by adding 10-minute or 20-minute delayed hepatobiliary phase images to the standard multiphase exam after gadoxetate disodium [8]. However, the liver specific contrast agents are still not widely used in clinical environment because of cost and extended exam time due to the acquisition of delayed hepatobiliary phases. Another, more practical approach to enhancing the detection of liver metastases is to explore the added clinical value of multiple arterial sub-phases acquisition in the diagnosis of hepatic metastases.

Recent technical progress in T1-weighted dynamic contrast MRI allows for the acquisition of multiple arterial phases in one breath hold (BH). Controlled aliasing in parallel imaging results in higher acceleration (CAIPIRINHA) is a novel acquisition scheme for volumetric imaging that modifies the image acquisition pattern to exploit sensitivity variations in the receiver coil array more efficiently, thereby improving the generalized auto-calibrating partially parallel acquisition (GRAPPA) performance [9,10], and allows further reductions in image acquisition time to 10 seconds for abdominal MRI by the use of higher acceleration factors. Time-resolved imaging with interleaved stochastic trajectories (TWIST) is amenable to time-resolved imaging with view sharing technique, and can also be combined with volumetric interpolated breath-hold examination (VIBE). Combining view sharing and the CAIPIRINHA technique allows for a further increase of the temporal resolution by maintaining the spatial resolution of the acquisition, theoretically facilitating dynamic, first-pass, contrast-enhanced imaging with high temporal resolution within a single breath hold. Homogeneous fat saturation is another major requirement for successful dynamic T1-weighted gradient-recalled echo (GRE) imaging of the abdomen. Dixon water-fat separation is virtually insensitive to B0 inhomogeneity [11,12]. The resulting CAIPIRINHA-Dixon-TWIST (CDT)–Volume-Interpolated Breath-Hold Examination (VIBE) is a new technique for fast dynamic 3-dimensional imaging of the abdomen with high spatial resolution [13,14].

The aim of this study was to assess lesion enhancement performance of the MA-CDT-VIBE protocol, with high spatial resolution ($1.3 \times 1.3 \times 3$ mm^3), high temporal resolution (2.64 seconds) and homogeneous fat suppression, for the detection of both hypo and hypervascular hepatic metastases at 3 T.

Material and Methods

Patient Population

All patients with known primary malignant tumor who had undergone an abdominal MR study from October 23, 2014, to January 15, 2015, were included. The inclusion criteria of this retrospective study were (1) optimum image quality; (2) confirmed hepatic metastases, by surgery or follow up CT/MRI and CEA levels for more than 4 months. The institutional review board waived the requirement of informed patient consent. The patient's population consisted of 31 individuals (mean age, 56.4 ± 9.9 years; range, 32-76 years; 14 male, 17 female) with a total of 109 hepatic metastases lesions. Diagnosis was confirmed by histopathological examination of surgical specimens in 7 patients. In the remaining 24 patients diagnosis was confirmed on CT or MRI if the lesions appeared compared to prior studies, or if lesions demonstrated regression in size with chemotherapy as compared with prior studies. Incidental benign liver lesions that were detected in these patients were not analyzed.

MR Acquisition

All examinations were acquired on a 3T MR scanner (MAGNETOM Skyra, Siemens Healthcare, Erlangen, Germany) with an 18-element body matrix coil and inbuilt 32-element spine matrix coil. The patients were positioned head first supine.

An MR-compatible automated injector pump (Spectris Solaris EP; Medrad, Indianola, PA) was used to administer the contrast agent through a 20-gauge antecubital intravenous site. After injection of 0.1 mmol/(kg body weight) of amacrocyclic Gd-DOTA contrast agent (Dotarem; Guerbet, Paris, France) at 2.5 ml/s, a 30-ml saline chaser at the same injection rate followed. Acquisition of the arterial phases using a non-product CDT-VIBE sequence was thus started 12 seconds after the start of the contrast injection and lasted for 22 seconds. After 15 seconds of free breathing, the portal venous phases of CDT-VIBE were acquired. Then, the delayed phase was acquired at 100 seconds, 150 seconds after the start of the contrast agent injection (Figure 1, Table 1).

Image Processing

A set of images which included the mean of all 6 hepatic arterial sub-phases was generated using the water-only images. In addition, 3 subtraction images were generated, including subtractions between hepatic 4th/6 and 1st/6 arterial sub-phases, 5th/6 and 1st/6 arterial sub-phases, 6th/6 and 1st/6 arterial sub-phases, respectively. This was performed to enhance lesion visualization. Eleven datasets which includes 6 hepatic arterial sub-phases, 1 set of the mean of above 6 hepatic arterial sub-phases, 3 subtraction sets, which was generated by Siemens Multi Workstation MMWP VE4.0, and the portal venous phase were presented for image analysis.

Image Analysis

Image analysis was performed by 2 independent reviewers (radiologists with 9 and 6 years of experience in body MRI) who assessed all 11 sets of images. Reviewers ranked each lesion from 1 to 11 based on lesion enhancement on all 11 sets of images. Scores of 1 to 4, 5 to 7, 8 to 10, and 11 were considered poor, acceptable, good, and excellent, respectively. For a comparison to the conventional single arterial phase, a second scanning was not performed. Instead, the equivalent-to-conventional single arterial phase was considered to be equal to the 3rd/6 arterial phase, as described by Kazmierczak et al. [14]. Furthermore, the mean of 6 arterial phases was included as an alternative for the equivalent-to-conventional single breath-hold arterial phase.

The third reviewer (radiologist with 17 year experience) carefully placed ROI on each lesion and on background liver parenchyma for sample Lesion ROI was slightly smaller than the size of the lesion to ensure that no surrounding normal parenchyma was included. ROIs placed on the hepatic parenchyma measure 0.5 to 2 cm and were carefully placed so as not to include hepatic vessels. Lesion to parenchymal enhancement curve was plotted for all lesions.

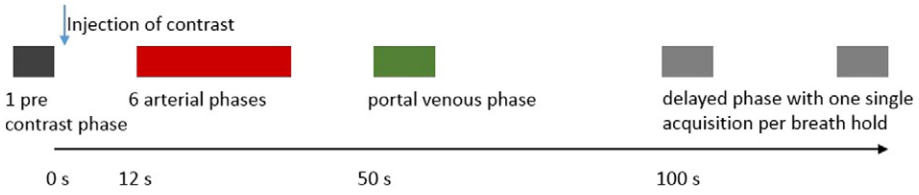

Figure 1. Multiple-breath-hold CDT-VIBE protocol for liver metastasis detection. The 6 arterial phases were acquired in a single breath hold, which were followed a single breath-hold portal venous phase and delayed phases.

Table 1. Sequence Parameters of MA-VIBE for 6 Sub-Phases in One Breath-Hold

Parameter	
FOV (mm^3)	380 × 295 × 192
Resolution (mm^3)	1.3 × 1.3 × 3.0
Parallel imaging	CAIPIRINHA: 2 × 2–1
TR/TE1, TE2 (ms)	4.29/1.31, 2.54
Flip angle (degree)	12
Fat suppression	2-point Dixon method
TWIST (A/B)	20% / 25%
Dynamic reconstruction mode	Forward share
Acquisition time (s)	22
Preparation time (s)	2.50
Total matrix acquisition time (s)	7.20
Temporal resolution (s)	2.64

Statistical Analysis

Statistical analyses were performed using SPSS 20.0. Inter-reviewer agreement was performed by kappa test. The phases with good (score 8–10) and excellent (score 11) lesion visualization were identified, and the number of lesions seen on each of these phases was compared to the number of lesions seen best on the equivalent-to-conventional single arterial phase as well as to those that were see best on the mean of 6 hepatic arterial sub-phases. Inter-reader agreement was also calculated. $P < .05$ was considered statistically significant.

Table 2. Patient Clinical Characteristics

No.	Sex	Age	Size(mm)		Metastasis Origin	Number of Lesions	Blood Supply (1 Hyper; 2 Hypo)
			Mean	Range			
1	F	61	10.1		Endometrial carcinoma	1	1
2	F	65	15.7	11.9–19.6	Breast cancer	7	1
3	F	49	10.9	8.0–15.9	Breast cancer	6	2
4	M	46	12.2	7.5–16.8	Colorectal carcinoma	2	1
5	F	51	10.8	6.8–16.8	Breast cancer	4	1
6	F	51	15.5		Breast cancer	1	2
7	F	55	4.7		Colorectal carcinoma	1	1
8	M	58	51.6		Colorectal carcinoma	1	1
9	M	59	8.7	5.6–11.7	Colorectal carcinoma	2	2
10	F	32	12.5		Breast cancer	1	1
11	F	64	5.8		Breast cancer	1	1
12	F	59	43.1		Colorectal carcinoma	1	1
13	F	49	15.4	8.65–26.7	Colorectal carcinoma	4	1
14	F	55	23.8	15.8–30.1	Breast cancer	4	1
15	F	59	26.8	16.1–40.1	Breast cancer	5	1
16	M	57	23.1	8.9–30.9	Colorectal carcinoma	8	1
17	M	67	23.0		Lung cancer	1	1
18	F	32	22.7	16.6–28.7	Breast cancer	2	1
19	M	57	20.8	16.1–27.7	Pancreatic cancer	4	1
20	M	68	20.6	7.6–31.4	Gastric cancer	8	1
21	M	61	25.7	11.8–35.7	Breast cancer	8	1
22	M	61	24.6	20.3–28.9	Colorectal carcinoma	2	1
23	M	71	13.2		Colorectal carcinoma	1	1
24	M	58	31.0	24.4–39.8	Colorectal carcinoma	3	1
25	F	67	29.3	27.6–30.9	Breast cancer	2	2
26	F	44	18.2	6.9–30.5	Breast cancer	9	1
27	M	59	15.8	9.7–19.6	Pancreatic cancer	6	1
28	F	57	17.5	8.7–55.0	Breast cancer	11	1
29	F	42	10.0		Breast cancer	1	1
30	M	55	8.1		Colorectal carcinoma	1	2
31	M	76	26.3		Colorectal carcinoma	1	2

Results

A total of 31 patients with 109 lesions were enrolled into this study, and patient demographics are shown in Table 2. The mean number of hepatic metastases per patient was 3 (range, 1-11 metastases). The maximum transverse diameter of hepatic metastases ranged from 5 to 55 mm.

Lesion Enhancement Evaluation

There were 96 hypervascular lesions, and 13 hypovascular lesions included for enhancement evaluation as detailed in Tables 2, 3. The color coded score maps ranked by 2 reviewers were shown in Figure 2*A* for all hypo and hypervascular lesions, and the inter-reviewer agreement was good for hypervascular lesions (kappa = 0.627, $P < .0001$) and excellent for hypovascular lesions (kappa = 1.0, $P < .0001$) respectively.

For the hypovascular lesions, the portal venous phase demonstrated the highest score for all 13 lesions, as shown in the bottom panel of Figure 2*B*. The 5th/6 and 6th/6 arterial phase followed (upper panel

Table 3. Number of Hypo and Hypervascular Lesions Best Seen on Each Set for the 2 Reviewers

	Reviewer I		Reviewer 2	
	Lesions Scoring 8-10	Lesions Scoring 11	Lesions Scoring 8-10	Lesions Scoring 11
Hypovascular Lesions (n = 13)				
Image set 1	0	0	0	0
Image set 2	0	0	0	0
Image set 3	0	0	0	0
Image set 4	7	0	8	0
Image set 5	12	0	13	0
Image set 6	12	0	13	0
Image set 7	3	0	2	0
Image set 8	1	0	0	0
Image set 9	1	0	0	0
Image set 10	3	0	2	0
Image set 11	0	13	0	13
Hypervascular Lesions (n = 96)				
Image set 1	0	0	1	0
Image set 2	0	0	2	0
Image set 3	5	3	26	2
Image set 4	4	12	51	6
Image set 5	81	1	67	15
Image set 6	25	56	33	44
Image set 7	11	0	8	0
Image set 8	24	4	23	0
Image set 9	44	4	36	7
Image set 10	50	12	33	15
Image set 11	2	4	8	7

Eleven datasets which includes 6 hepatic arterial sub-phases (sets 1-6), 1 set of the mean of above 6 hepatic arterial sub-phases (set 7), 3 subtraction sets (sets 8-10), and the portal venous phase (set 11).

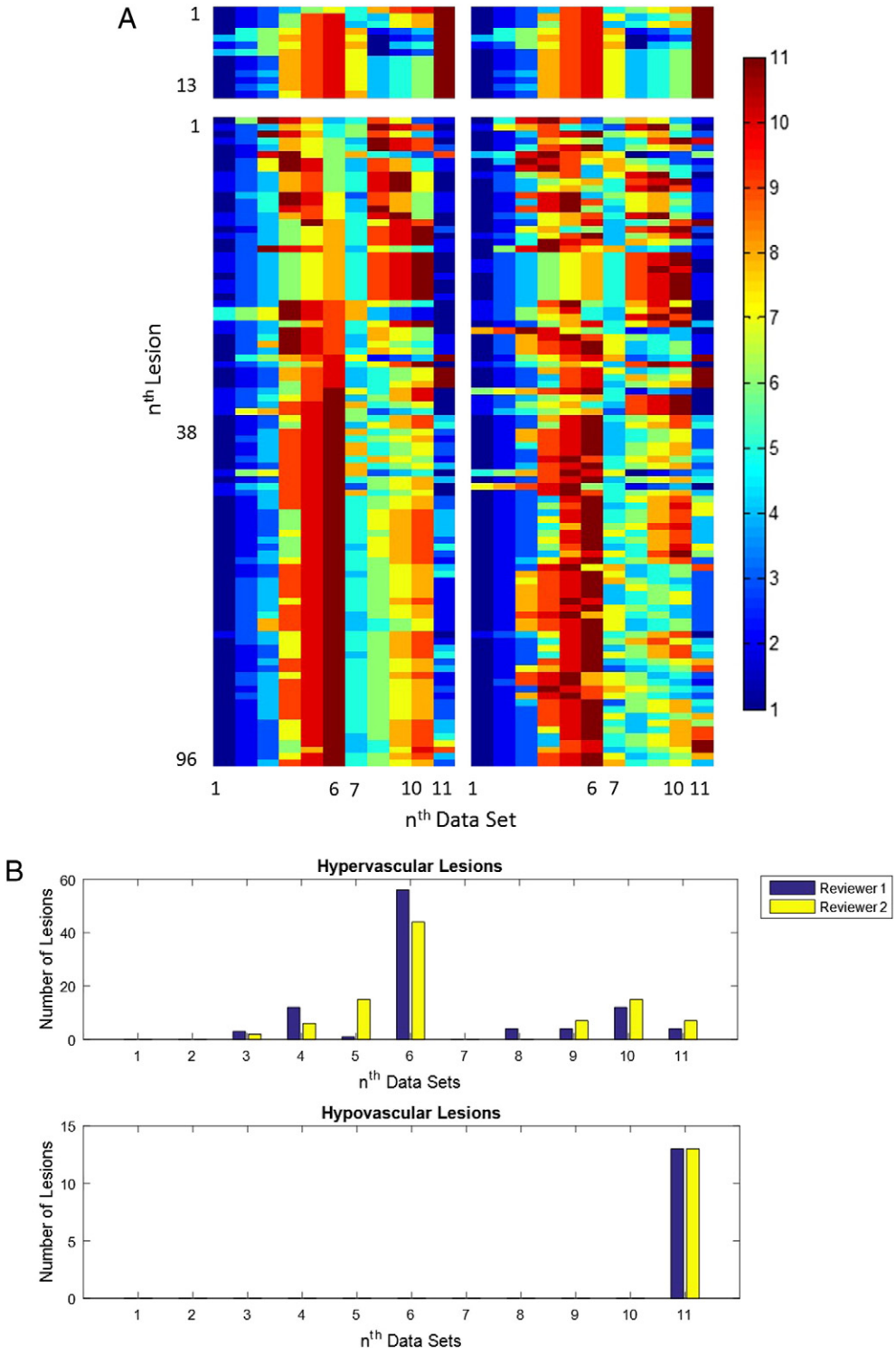

Figure 2. (A) Score maps for all hypovascular lesions (total number: 13, upper panels) and all hypervascular lesions (total number: 96, bottom panels) as scored by two reviewers (left panels: reviewer 1; right panels: reviewer 2). The y axis of map refers to the lesion number, and the x axis labels the evaluated image sets in the following order: 1 to 6 represent the 1st/6 to 6th/6 arterial phase, 7 represents the mean arterial phase, 8 to 10 represent the subtracted arterial phases (4th/6 – 1st/6 to 6th/6 – 1st/6), and 11 represent the portal venous phase. The score of visualizing each lesion ranges from 1 to 11, with 1 being the lowest (dark blue) and 11 being the highest (dark red). (B) The total number of lesions with only the highest score (score: 11) are counted for each data set for the 2 reviewers and are displayed in the histogram below (b).

of Figure 2*A* and Table 3), and they performed better than the equivalent-to-conventional arterial phase (3rd/6 arterial phase (P = .039 for both reviewers) and mean of 6 arterial phases (P = .03 and P < .001 for the 2 readers, respectively).

For the hypervascular lesions, the 6th/6 arterial phase demonstrated the highest score for 56 and 44 lesions, for readers 1 and 2, respectively. The 5th/6 arterial phase followed for 81 and 67 lesions, for readers 1 and 2, respectively. Only 3 and 2 lesions scored excellent

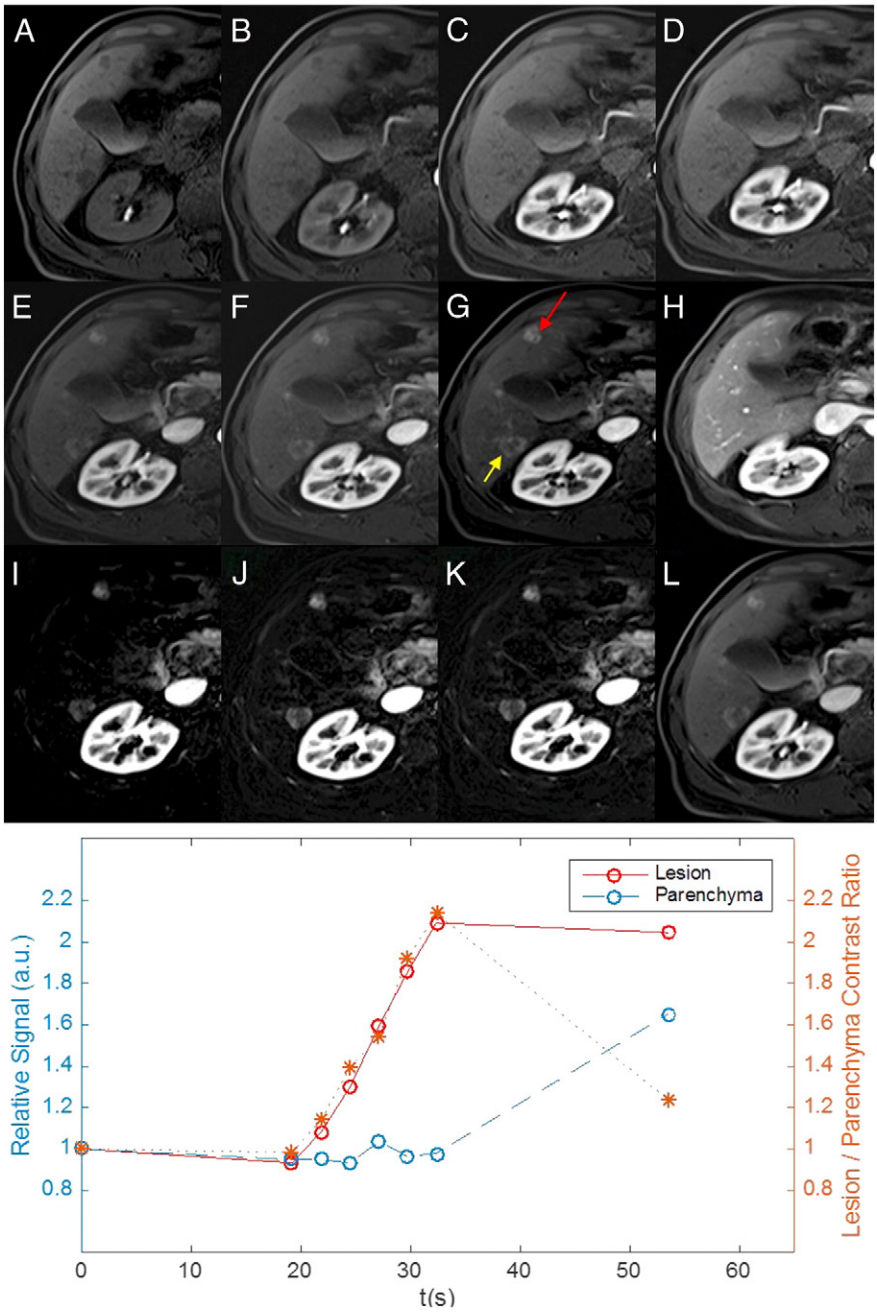

Fig. 3. Hepatic arterial contrast dynamics of liver metastases from primary colon cancer in a 61-year-old male. Precontrast images (A), CDT-VIBE 6 arterial phases at 19.20 seconds (B, 1st/6), 21.84 seconds (C, 2nd/6), 24.48 seconds (D, 3rd/6), 27.12 seconds (E, 4th/6), 29.72 seconds (F, 5th/6), and 32.36 seconds (G, 6th/6), portal venous phase (H), subtracted arterial phases between 4th/6 and 1st/6 (I), 5th/6 1st/6(J), 6th/6 and 1st/6 (K), mean of 6 arterial phases (L). The hepatic arterial enhancement of lesion (red arrow) is the strongest at 32.36 seconds after contrast injection (G). A second lesion in the post right lobe (yellow arrow) has similar enhancement characteristics. Plot of dynamic contrast enhancement curve of lesion (solid red) (red arrow), hepatic parenchyma (dashed blue) and lesion-to-parenchyma contrast ratio (dotted orange) using 6 arterial phases and portal venous phase.

(score = 11) on the 3rd/6 arterial sub-phase, for the 2 readers, respectively (Table 3). No lesion scored excellent (11) on the 7th set (mean of above 6 hepatic arterial sub-phases). 11 and 8 lesions scored good (8–10) for the 2 readers, respectively. The difference between the number of lesions which scored 11 on the 6th/6 phase and the 3rd/6 phase was statistically significant (t test, $P < .0001$ for both readers). The difference between the number of lesions which scored 11 on the 6th/6 phase and set of the mean of above 6 hepatic arterial sub-phases was statistically significant (t test, $P < .0001$ for both readers).

Discussion

This study shows the incremental value of 6 hepatic arterial phases obtained using CDT-VIBE for hepatic metastases, compared to the equivalent-to-conventional single arterial phase. Conventional imaging approaches are performed with a hepatic arterial phase that may be difficult to optimize, or fail in the case of the fast wash-in and wash-out. CDT-VIBE allows for multiple arterial phases per breath-hold that provide a wide observation window for better arterial enhancement, especially for hypervascular metastasis.

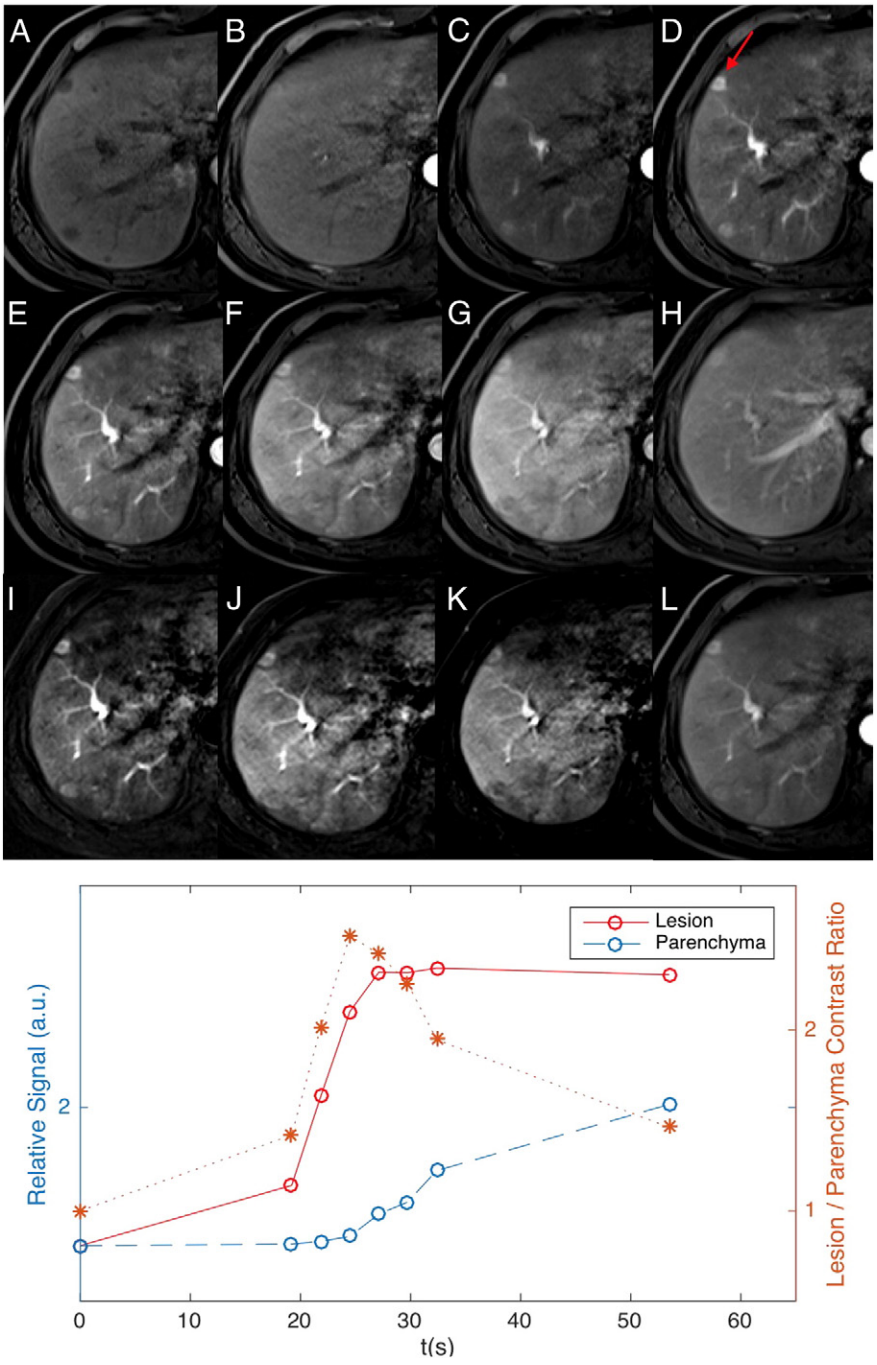

Fig. 4. Hypervascular liver metastases from primary gastric cancer in a 68-year-old male. Precontrast image (A), CDT-VIBE 6 arterial phases at 19.20 seconds (B, 1st/6), 21.84 seconds (C, 2nd/6), 24.48 seconds (D, 3rd/6), 27.12 seconds (E, 4th/6), 29.72 seconds (F, 5th/6), and 32.36 seconds (G, 6th/6), portal venous phase (H), subtracted arterial phases between 4th/6 and 1st/6 (I), 5th/6 and 1st/6(J), 6th/6 and 1st/6 (K), mean of 6 arterial phases (L). The hypervascular lesions (red arrow) enhanced strongest in 3rd/6 (D). Plot of dynamic contrast enhancement curve of lesion (solid red), hepatic parenchyma (dashed blue) and lesion-to-parenchyma contrast ratio (dotted orange) using 6 arterial phases and portal venous phase.

This finding is supported by the corresponding dynamic contrast enhancement curves of lesion, parenchyma and the lesion-to-parenchyma contrast ratio (Figures 2–5).

This study compared the 6 arterial phases and two types of the equivalent-to-conventional arterial phase including the mean of 6 arterial phases and the 3rd/6 arterial phase. Our data demonstrate that MA-CDT-VIBE performs better than two types of the equivalent-to-conventional single arterial phase in detecting the conspicuous metastasis lesions with improved lesion enhancement performance in arterial phases. In this study the highest enhancement of hypervascular hepatic metastases occurred in 6th/6 phase of enhancement (32.36 seconds), where 56/96 and 44/96 lesions scored excellent (score = 11) by reader 1 and reader 2, respectively. Good lesion visualization was recorded in 5th/6 phase of enhancement (29.72 seconds), where 81/96 and 67/96 lesions scored good (score 8–10) by reader 1 and reader 2, respectively (Table 3; Figures 3 and 4).

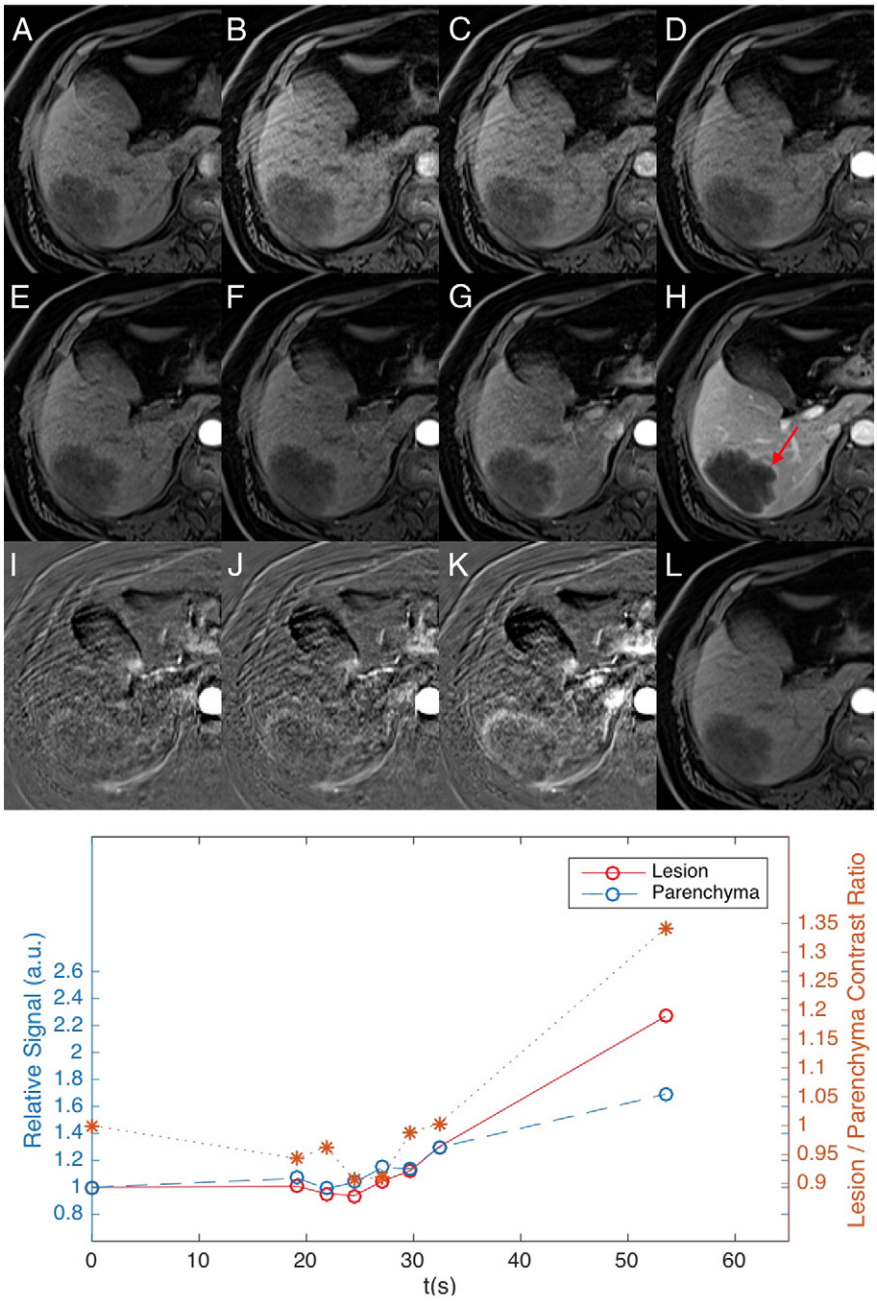

Fig. 5. Hypovascular liver metastases from primary breast cancer in a 49-year-old female. Precontrast images (A), CDT-VIBE 6 arterial phases at 19.20 seconds (B, 1st/6), 21.48 seconds (C, 2nd/6), 24.48 seconds (D, 3rd/6), 27.12 seconds (E, 4th/6), 29.72 seconds (F, 5th/6), and 32.36 seconds (G, 6th/6), portal venous phase (H), subtracted arterial phases between 4th/6 and 1st/6 (I), 5th/6 and 1st/6(J), 6th/6 and 1st/6 (K), mean of 6 arterial phases (L). The hypovascular lesion with rim enhancement pattern (red arrow) can be identified on 5th/6 (F), 6th/6 (G), and portal venous phase (H). Plot of dynamic contrast enhancement curve of lesion (solid red), parenchyma (dashed blue) and lesion-to-parenchyma contrast ratio (dotted orange) using 6 arterial phases and portal venous phase.

Precise timing of the hepatic artery is essential and important for correct tumor detection, choice of treatment plan depending on the status of tumor blood supply, and treatment response monitoring. Conventional imaging approaches are performed with a single hepatic arterial phase that may be suboptimum in capturing peak arterial enhancement. Currently, although several technical approaches for an optimal timing of the hepatic arterial phase are available, for example, scanning at fixed time points, a prescan test bolus or real-time bolus tracking [15,16], no consensus on what vascular reference point to use has been reached for the latter techniques [14].

Kent et al. [17] reported 84/113 (74%) liver metastases that were hypovascular on CT were hypervascular on angiography. Noboru et al. [18] analyzed hemodynamics of liver metastasis based on hepatic arteriography by single-level Dynamic CT, and found that the time of appearance of rim enhancement in 3 of 10 hypervascular nodules (30%) was <10 s and was ≥10 s in the remaining 7 nodules. On the other hand, the time of appearance of rim enhancement was <10 s in 17 of 18 nodules (94%) of hypovascular metastasis ($P < .01$). However, in fact, it is impossible to acquire the whole liver CT images with more than 3 hepatic artery phases with more radiation.

Philippe et al. reported that the portal-dominant phase is the most sensitive of the three helical CT imaging phases in the preoperative evaluation of patients with hypovascular hepatic metastases because it allows depiction of significantly more hepatic metastases than any of the other phases [19]. This is also supported by our study with highest visualization of hypovascular hepatic metastases occurred in the portal venous phase of enhancement (53.50 seconds), where13/13 lesions scored excellent (score = 11) by both readers 1.

Recently, DWI and hepatobiliary phase MRI with new hepatobiliary contrast agents have demonstrated improved sensitivity over routine MRI alone for the detection of hepatic metastases [20], and especially improved detection of small (<1 cm) lesions [8]. However, the hepatobiliary contrast agents are relative expensive, and DWI does not show the status of vascularity.

The limitation for the current study includes lack of pathologic confirmation of all the reported lesions. However, the reference standard we used for determining the number of hepatic metastases was the combination of surgical examination or the features of MRI with the known primary malignant tumor and follow-up examinations. Another limitation of this study is the limited number of hypovascular lesions (13 lesions). However, the result still showed that MA-CDT-VIBE was able to demonstrate more arterial information for poor blood supply hepatic metastases (Figure 5). Kent et al. [17] reported 84/113 (74%) liver metastases that were hypovascular on CT were hypervascular on angiography. In the future it would be interesting to compare CDT-VIBE and angiography. Finally, we did not perform a separated conventional single arterial phase scan. Comparison with an additional arterial standard VIBE sequence would necessitate a second MRI examination with an additional administration of contrast media in a different day, which was clinically not indicated. However, the mean of 6 arterial phases was included as an alternative for the equivalent-to-conventional single breath-hold arterial phase, and from the contrast bolus timing perspective, the 3rd of 6 arterial sub-phases was reasonably equivalent to the conventional single hepatic arterial phase.

Conclusion

Overall, MA-CDT-VIBE MRI of the liver is showing the higher performance over the two types of equivalent-to-conventional single arterial phase exams in providing an optimized wide observing window for tumor vascularity evaluation. This might be essential for the accurate detection and assessment of the true burden of hepatic metastases at the time of first diagnosis. This could significantly determine the choice of therapeutic approach and could impact patient outcome.

References

[1] Baker ME and Pelley R (1995). Hepatic metastases: basic principles and implications for radiologists. *Radiology* **197**(2), 329–337. http://dx.doi.org/10.1148/radiology.197.2.7480672.

[2] Charnsangavej C, Clary B, Fong Y, Grothey A, Pawlik TM, and Choti MA (2006). Selection of patients for resection of hepatic colorectal metastases: expert consensus statement. *Ann Surg Oncol* **13**(10), 1261–1268. http://dx.doi.org/10.1245/s10434-006-9023-y.

[3] Frankel TL, Gian RK, and Jarnagin WR (2012). Preoperative imaging for hepatic resection of colorectal cancer metastasis. *J Gastrointestin Oncol* **3**(1), 11–18. http://dx.doi.org/10.3978/j.issn.2078-6891.2012.002.

[4] Niekel MC, Bipat S, and Stoker J (2010). Diagnostic imaging of colorectal liver metastases with CT, MR imaging, FDG PET, and/or FDG PET/CT: a meta-analysis of prospective studies including patients who have not previously undergone treatment. *Radiology* **257**(3), 674–684. http://dx.doi.org/10.1148/radiol.10100729.

[5] Sahani DV, Kalva SP, Fischman AJ, Kadavigere R, Blake M, Hahn PF, and Saini S (2005). Detection of liver metastases from adenocarcinoma of the colon and pancreas: comparison of mangafodipir trisodium-enhanced liver MRI and whole-body FDG PET. *AJR Am J Roentgenol* **185**(1), 239–246. http://dx.doi.org/10.2214/ajr.185.1.01850239.

[6] Chan VO, Das JP, Gerstenmaier JF, Geoghegan J, Gibney RG, Collins CD, Skehan SJ, and Malone DE (2012). Diagnostic performance of MDCT, PET/CT and gadoxetic acid (Primovist((R)))-enhanced MRI in patients with colorectal liver metastases being considered for hepatic resection: initial experience in a single centre. *Ir J Med Sci* **181**(4), 499–509. http://dx.doi.org/10.1007/s11845-012-0805-x.

[7] Ward J, Robinson PJ, Guthrie JA, Downing S, Wilson D, Lodge JP, Prasad KR, Toogood GJ, and Wyatt JI (2005). Liver metastases in candidates for hepatic resection: comparison of helical CT and gadolinium- and SPIO-enhanced MR imaging. *Radiology* **237**(1), 170–180. http://dx.doi.org/10.1148/radiol.2371041444.

[8] Jeong HT, Kim MJ, Park MS, Choi JY, Choi JS, Kim KS, Choi GH, and Shin SJ (2012). Detection of liver metastases using gadoxetic-enhanced dynamic and 10- and 20-minute delayed phase MR imaging. *J Magn Reson Imaging* **35**(3), 635–643. http://dx.doi.org/10.1002/jmri.22880.

[9] Breuer FA, Blaimer M, Mueller MF, Seiberlich N, Heidemann RM, Griswold MA, and Jakob PM (2006). Controlled aliasing in volumetric parallel imaging (2D CAIPIRINHA). *Magn Reson Med* **55**(3), 549–556. http://dx.doi.org/10.1002/mrm.20787.

[10] Breuer FA, Blaimer M, Heidemann RM, Mueller MF, Griswold MA, and Jakob PM (2005). Controlled aliasing in parallel imaging results in higher acceleration (CAIPIRINHA) for multi-slice imaging. *Magn Reson Med* **53**(3), 684–691. http://dx.doi.org/10.1002/mrm.20401.

[11] Dixon WT (1984). Simple proton spectroscopic imaging. *Radiology* **153**(1), 189–194. http://dx.doi.org/10.1148/radiology.153.1.6089263.

[12] Michaely HJ, Attenberger UI, Dietrich O, Schmitt P, Nael K, Kramer H, Reiser MF, Schoenberg SO, and Walz M (2008). Feasibility of gadofosveset-enhanced steady-state magnetic resonance angiography of the peripheral vessels at 3 Tesla with Dixon fat saturation. *Invest Radiol* **43**(9), 635–641. http://dx.doi.org/10.1097/RLI.0b013e31817ee53a.

[13] Michaely HJ, Morelli JN, Budjan J, Riffel P, Nickel D, Kroeker R, Schoenberg SO, and Attenberger UI (2013). CAIPIRINHA-Dixon-TWIST (CDT)-volume-interpolated breath-hold examination (VIBE): a new technique for fast time-resolved dynamic 3-dimensional imaging of the abdomen with high spatial resolution. *Invest Radiol* **48**(8), 590–597. http://dx.doi.org/10.1097/RLI.0b013e318289a70b.

[14] Kazmierczak PM, Theisen D, Thierfelder KM, Sommer WH, Reiser MF, Notohamiprodjo M, and Nikolaou K (2015). Improved detection of hypervascular liver lesions with CAIPIRINHA-Dixon-TWIST-volume-interpolated breath-hold examination. *Invest Radiol* **50**(3), 153–160. http://dx.doi.org/10.1097/RLI.0000000000000118.

[15] Sharma P, Kitajima HD, Kalb B, and Martin DR (2009). Gadolinium-enhanced imaging of liver tumors and manifestations of hepatitis: pharmacodynamic and technical considerations. *Top Magn Reson Imaging* **20**(2), 71–78. http://dx.doi.org/10.1097/RMR.0b013e3181c42454.

[16] Earls JP, Rofsky NM, DeCorato DR, Krinsky GA, and Weinreb JC (1996). Breath-hold single-dose gadolinium-enhanced three-dimensional MR aortography: usefulness of a timing examination and MR power injector. *Radiology* **201**(3), 705–710. http://dx.doi.org/10.1148/radiology.201.3.8939219.

[17] Sato KT, Omary RA, Takehana C, Ibrahim S, Lewandowski RJ, Ryu RK, and Salem R (2009). The role of tumor vascularity in predicting survival after yttrium-90 radioembolization for liver metastases. *J Vasc Interv Radiol* **20**(12), 1564–1569. http://dx.doi.org/10.1016/j.jvir.2009.08.013.

[18] Terayama N, Matsui O, Ueda K, Kobayashi S, Sanada J, Gabata T, Kawamori Y, and Kadoya M (2002). Peritumoral rim enhancement of liver metastasis: hemodynamics observed on single-level dynamic CT during hepatic arteriography and histopathologic correlation. *J Comput Assist Tomogr* **26**(6), 975–980.

[19] Soyer P, Poccard M, Boudiaf M, Abitbol M, Hamzi L, Panis Y, Valleur P, and Rymer R (2004). Detection of hypovascular hepatic metastases at triple-phase helical CT: sensitivity of phases and comparison with surgical and histopathologic findings. *Radiology* **231**(2), 413–420. http://dx.doi.org/10.1148/radiol.2312021639.

[20] Zech CJ, Herrmann KA, Reiser MF, and Schoenberg SO (2007). MR imaging in patients with suspected liver metastases: value of liver-specific contrast agent Gd-EOB-DTPA. *Magn Reson Med Sci* **6**(1), 43–52.